Applied Physics Express 6 (2013) 061003
http://dx.doi.org/10.7567/APEX.6.061003

Epitaxial Growth of III–Nitride/Graphene Heterostructures for Electronic Devices

Neeraj Nepal[1], Virginia D Wheeler[1], Travis J Anderson[1], Francis J Kub[1], Michael A Mastro[1], Rachael L Myers-Ward[1], Syed B Qadri[2], Jaime A Freitas[1], Sandra C Hernandez[3], Luke O Nyakiti[1], Scott G Walton[3], Kurt Gaskill[1], and Charles R Eddy, Jr.[1]

[1]Electronics Science and Technology Division, U.S. Naval Research Laboratory, Washington, D.C. 20375, U.S.A.
[2]Material Sciences and Technology Division, U.S. Naval Research Laboratory, Washington, D.C. 20375, U.S.A.
[3]Plasma Physics Division, U.S. Naval Research Laboratory, Washington, D.C. 20375, U.S.A.

Received April 17, 2013; accepted May 23, 2013; published online June 7, 2013

Epitaxial GaN films were grown by metal organic chemical vapor deposition (MOCVD) on functionalized epitaxial graphene (EG) using a thin (~11 nm) conformal AlN nucleation layer. Raman measurements show a graphene 2D peak at 2719 cm^{-1} after GaN growth. X-ray diffraction analysis reveals [0001]-oriented hexagonal GaN with (0002) peak rocking curve full width at the half maximum (FWHM) of 544 arcsec. The FWHM values are similar to reported values for GaN grown by MOCVD on sapphire. The GaN layer has a strong room-temperature photoluminescence band edge emission. Successful demonstration of GaN growth on EG opens up the possibility of III–nitride/graphene heterostructure-based electronic devices and promises improved performance. © 2013 The Japan Society of Applied Physics

For high-speed current switching applications, hot electron transistors (HETs) are superior to all other types of devices with cut-off frequencies greater than 1 THz.[1,2] The typical state-of-the-art HET base layer consists of either a heavily doped semiconductor or metal. In HETs with a heavily doped semiconductor base, the ballistic or quasiballistic transportation of hot electrons is inhibited by impurity and carrier-carrier scattering.[3] Whereas for HETs with a metal base, the quantum mechanical reflection at the interface between metal and semiconductor partially prevents a hot electron from being transmitted to the collector region, which limits the device performance.[4] Clearly, it is desirable to replace the typical base layer with a material that does not suffer from the above problems. Here, we propose replacing the base layer with graphene since it should overcome the limitations noted above and enable cut-off frequencies in excess of 1 THz.[5,6] Furthermore, we demonstrate that III–V HET structures can be epitaxially grown on a graphene base using a graphene fluorine-functionalization approach that does not appreciably disrupt the graphene lattice.[7,8] We further show, for the first time, that the resulting quality of the III–V nitride layers is similar to that obtained by traditional growth methods on traditional III–V nitride substrates.

Previously, Kunook et al. grew GaN on oxygen-plasma-treated graphene,[9] which resulted in a polycrystalline GaN layer with a rough and irregular surface. Additionally, they explored the use of vertically aligned ZnO nanowalls as an intermediate layer on oxygen plasma treated graphene to grow GaN-based light emitting diodes (LEDs). The oxidized graphene and complex semiconductor interface of such an approach are certain to present significant trap centers for carriers, and hence degrade the performance of the heterojunction. Thus, the ability to grow semiconductor-quality III–nitrides directly on the graphene with minimal interface defects is essential for such applications. Despite several efforts to deposit high-κ dielectrics on graphene,[10,11] the successful growth of a high-quality III–nitride film on graphene has not been reported yet. However, there is information regarding the band line up for this system through the work of Zhong et al., who studied the electrical behavior of exfoliated graphene on n- and p-type GaN films.[12] They reported that the single-layer graphene adapts its Fermi level toward the semiconductor's Fermi level, which results in reduced barrier heights between graphene and both n- and p-type GaN.

The growth of III–nitrides directly on graphene is challenging as there are no dangling bonds on the surface of graphene to promote bonding with foreign atoms. As a result, various functionalization methods have been employed to modify the graphene surface to promote bond formation and create pristine dielectric/graphene interfaces without altering the advantageous graphene electronic properties.[8]

Fluorination, using xenon difluoride (XeF_2) gas at room-temperature, is one of the methods reported to functionalize the epitaxial graphene surface for enhanced dielectric deposition, which when optimized shows little to no degradation to the graphene lattice as measured by electronic transport.[7,8] In fact, an increase in graphene carrier mobility after the deposition of a thin high-κ oxide on fluorinated graphene using an optimal 6–7% areal percentage of C–F bonding has been shown. The chemisorption of a fluorine atom forming a unique semi-ionic C–F bond rather than a covalent bond to the graphene surface allows the structural and electrical integrity of the graphene to be preserved, while providing sufficient nucleation sites for subsequent high-quality layer deposition. Thus, fluorination via XeF_2 is the preferred functionalization method employed in this work.

High-temperature growth of III–nitride under conventional molecular beam epitaxy (MBE) or metal organic chemical vapor deposition (MOCVD) conditions (500–1300 °C) directly on functionalized graphene results in the complete desorption of the fluorine adatom and could hinder the advantage of fluorination; thus, a low-temperature albeit high-quality growth of a III–nitride nucleation layer is important. Atomic layer epitaxy (ALE) enables the growth of thin, uniform layers at low-temperatures needed to preserve the essential fluorine functional groups. The inherent kinetics of ALE allow the growth of crystalline materials at greatly reduced temperatures relative to standard epitaxial techniques such as MOCVD.[13,14] In this work, we report on the first ever epitaxial growth of III–nitride semiconductor layers on epitaxial graphene (EG) by using XeF_2 functionalization followed by an ALE III–nitride buffer layer; as will be shown, this is a key enabler for a range of new heterojunction devices.

EG was grown on 4° 4H-SiC ($16 \times 16\,mm^2$) samples using the Si sublimation method described elsewhere.[15] The synthesized EG layers were characterized using atomic force

 © 2013 The Japan Society of Applied Physics

Report Documentation Page			*Form Approved* *OMB No. 0704-0188*

Public reporting burden for the collection of information is estimated to average 1 hour per response, including the time for reviewing instructions, searching existing data sources, gathering and maintaining the data needed, and completing and reviewing the collection of information. Send comments regarding this burden estimate or any other aspect of this collection of information, including suggestions for reducing this burden, to Washington Headquarters Services, Directorate for Information Operations and Reports, 1215 Jefferson Davis Highway, Suite 1204, Arlington VA 22202-4302. Respondents should be aware that notwithstanding any other provision of law, no person shall be subject to a penalty for failing to comply with a collection of information if it does not display a currently valid OMB control number.

1. REPORT DATE **2013**	2. REPORT TYPE	3. DATES COVERED **00-00-2013 to 00-00-2013**
4. TITLE AND SUBTITLE **Epitaxial Growth of III-Nitride/Graphene Heterostructures for Electronic Devices**		5a. CONTRACT NUMBER 5b. GRANT NUMBER 5c. PROGRAM ELEMENT NUMBER
6. AUTHOR(S)		5d. PROJECT NUMBER 5e. TASK NUMBER 5f. WORK UNIT NUMBER
7. PERFORMING ORGANIZATION NAME(S) AND ADDRESS(ES) **Electronics Science and Technology Division,,U.S. Naval Research Laboratory,,Washington,DC,20375**		8. PERFORMING ORGANIZATION REPORT NUMBER
9. SPONSORING/MONITORING AGENCY NAME(S) AND ADDRESS(ES)		10. SPONSOR/MONITOR’S ACRONYM(S) 11. SPONSOR/MONITOR’S REPORT NUMBER(S)

12. DISTRIBUTION/AVAILABILITY STATEMENT

Approved for public release; distribution unlimited

13. SUPPLEMENTARY NOTES

14. ABSTRACT

15. SUBJECT TERMS

16. SECURITY CLASSIFICATION OF:			17. LIMITATION OF ABSTRACT	18. NUMBER OF PAGES	19a. NAME OF RESPONSIBLE PERSON
a. REPORT **unclassified**	b. ABSTRACT **unclassified**	c. THIS PAGE **unclassified**	**Same as Report (SAR)**	**5**	

Standard Form 298 (Rev. 8-98)
Prescribed by ANSI Std Z39-18

microscopy (AFM), LEO supra 55 scanning electron microscopy (SEM), Thermo Scientific K-Alpha X-ray photoelectron spectroscopy (XPS), and room-temperature Raman and photoluminescence measurements. The Raman characterization was performed using an InVia Raman microscope (Renishaw) equipped with a 50× objective lens, a 514.5 nm diode laser excitation, at a set power of 20 mW at the source with a spot size of 5 µm. Following initial characterization, the EG/SiC was patterned (disk with diameters of 50, 100, 200, and 500 µm) with SiN_x deposited by plasma-enhanced chemical vapor deposition using standard photolithography and liftoff techniques. The patterned EG was functionalized using six 30-s-long pulses of a XeF_2 plasma to form about 6–7% "semi-ionic" C–F bonds as described elsewhere.[8] The selectively functionalized graphene was then inserted into a Fiji ALE reactor (Cambridge NanoTech) heated resistively at 280 °C for the growth of the AlN nucleation layer of approximately 11 nm thickness. A Si(111) witness sample was used to monitor the growth rate. After pumping the reactor to its base vacuum of 166 mTorr, five pulses of 99.999% pure trimethylaluminum (TMA; ~1 Torr) (from Stream Chemicals) were introduced into the reactor to promote the reaction of the TMA molecule with fluorine sites on the EG surface, presumably creating more nucleation sites for AlN growth. The ALE growth of AlN was carried out in an Ar ambient. Each ALE cycle consisted of first a 60 ms TMA pulse. The TMA was added to 30 sccm flow of ultrahigh-purity (UHP) Ar carrier gas via the metal organic precursor line while 100 sccm of UHP Ar was introduced separately through the plasma source. For 30/100 sccm flow of UHP Ar, the reactor pressure was at 166 mTorr. Unreacted TMA precursor and by-products were removed by purging the chamber with UHP Ar for 10 s. A 15-s-long, 150 W UHP N_2 plasma pulse was used as a nitrogen precursor. To remove unreacted nitrogen precursors and by-products, the deposition chamber was purged again with UHP Ar for 10 s. The complete AlN growth consisted of 150 cycles, resulting in an AlN thickness of 11 nm on the Si witness sample as measured by spectroscopic ellipsometry. An AFM operating in tapping mode was used to verify the uniformity of the AlN. After characterization of the ALE-grown AlN/EG, the sample was transferred into an MOCVD reactor. Unintentionally doped GaN of targeted thickness of 800 nm was grown in a heavily modified vertical impinging flow MOCVD reactor (CVD, Inc.) with a rotating susceptor. Chemical bonding within the GaN/AlN/graphene/SiC stack (GaN/graphene) was characterized by XPS using a monochromatic Al ($K\alpha$ = 1486.6 eV) source and spot size of 0.4 mm. Raman spectra were acquired using an argon laser (514.5 nm) with 5 µm spot size as an excitation source on the final structure. The crystalline quality was characterized using a double-crystal X-ray diffractometer in both in-plane and out-of-plane directions. Photoluminescence (PL) measurement was carried out using a HeCd laser at 325 nm, 1800 gr/mm double-grating spectrometer, fitted with a UV-sensitive photomultiplier tube.

Several initial attempts were made to grow MOCVD GaN directly on unfunctionalized EG, which always resulted in a non-uniform distribution of individual GaN crystallites instead of a continuous film. Based on previous work,[8] we hypothesized that using fluorination with XeF_2 significantly increases the density of nucleation sites, which would subsequently promote uniform, epitaxial growth. To ensure that such functionalization survives to promote nucleation, a low-temperature epitaxial growth process is required at least at the beginning of the heteroepitaxy process, which in this case is the ALE of AlN. Hence, the rest of this paper will focus on our approach of using a fluorine-functionalized EG surface to enable a thin ALE AlN buffer layer for subsequent thick GaN growth.

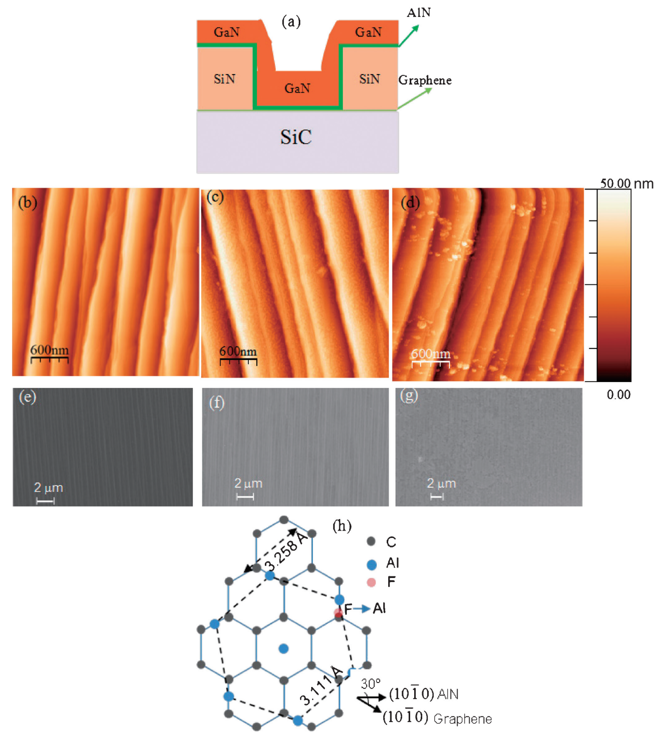

Fig. 1. (a) Schematic showing the GaN/AlN/graphene/SiC layered structure, (b) AFM image as-synthesized epitaxial graphene, (c) AFM image of 1.2 nm ALE AlN/graphene, (d) AFM image of GaN/graphene, (e) SEM image of pristine graphene, (f) SEM image of 1.2 nm ALE AlN/graphene, (g) SEM image of GaN on AlE AlN/graphene. (h) Al atoms replace F atoms creating an AlN nucleation site on graphene resulting in the proposed crystalline alignments. The proposed lattice mismatch between AlN and graphene is 4.5%.

Thin conformal AlN and GaN layers were grown as shown in the layered structure in Fig. 1(a). The starting pristine graphene was about 4–5 layers thick and it follows the surface morphology of the underlying SiC, with step edges and terraces as shown in AFM and SEM images in Figs. 1(b) and 1(e), respectively. Under optimized ALE growth conditions, AlN is deposited uniformly on EG; AFM and SEM images of 1.2 nm AlN on XeF_2 functionalized EG in Figs. 1(c) and 1(f) show uniform nucleation. Figures 1(d) and 1(g) show AFM and SEM images of epitaxial GaN on EG using an 11 nm ALE AlN as a nucleation layer. In Fig. 1(h), we propose the AlN lattice alignment along *m*-plane to fluorinated graphene replacing a semi-ionically bound F atom by an Al atom without damaging the graphene lattice. The lattice mismatch between graphene and AlN is 4.5%, which is significantly smaller than the 13% between AlN and sapphire (which is the most commonly used substrate for III–nitride growth), and should lead to less defects forming during heteroepitaxial

© 2013 The Japan Society of Applied Physics

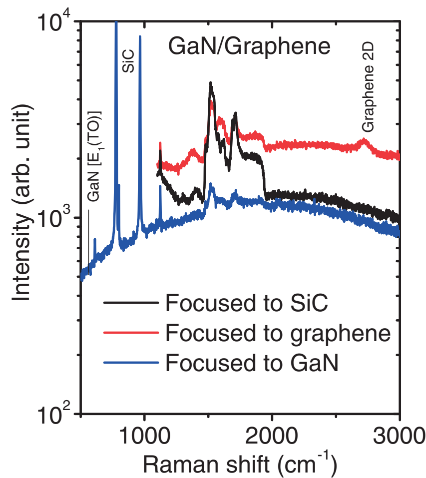

Fig. 2. Raman spectra of GaN/AlN/graphene/SiC stack when the laser was focused within (a) SiC (black line), (b) graphene (red line), and (c) GaN (blue line). Note the graphene 2D peak at 2719 cm^{-1} for (c).

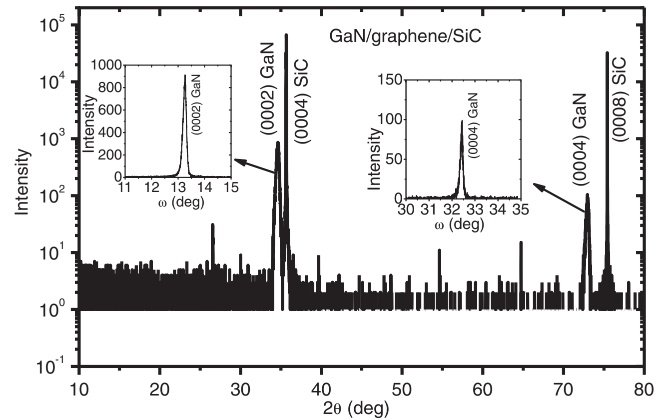

Fig. 3. XRD peaks from the GaN/AlN/graphene/SiC stack. Insets show the rocking curve of GaN(0002) and (0004) reflections. Rocking curve FHWMs of (0002) and (0004) peaks are 544 and 461 arcsec, respectively.

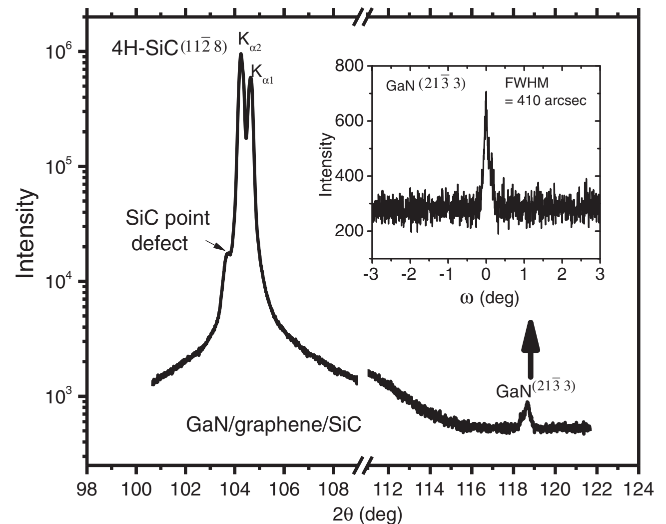

Fig. 4. Asymmetric XRD peaks from the GaN/AlN/graphene/SiC stack. Inset shows the rocking curve of GaN(21$\bar{3}$3) reflection. Rocking curve FHWM of (21$\bar{3}$3) peak is 410 arcsec.

growth of thin layers. After targeted 800 nm growth of GaN by MOCVD on the thin ALE AlN nucleation layer, step edges and terraces are still clearly visible [Fig. 1(d)], which suggests uniform two-dimensional (2D) growth of GaN. The few particles seen on the surface may be due to island nucleation. Additionally, the SEM image in Fig. 1(g) suggests a uniform and almost pinhole-free surface morphology of the GaN on graphene over large areas that would be required to achieve higher device yields.

To assess if the graphene remains underneath the GaN, Raman spectra were taken on the final structure (GaN/AlN/graphene/SiC) and shown in Fig. 2. As the GaN is relatively transparent to the pump wavelength, when the laser was focused on the underlying graphene, the 2D peak at 2719 cm^{-1} is clearly visible, implying that, although the GaN growth process involved several different graphene surface processing steps, the graphene layer was preserved. This confirms that the AlN and GaN growth were on graphene, not on the SiC. When the laser is focused on the SiC, the graphene peak disappears. There is no clear GaN peak, as it may be buried under the SiC background Raman signal.

The crystalline quality and orientation of the GaN on EG was assessed using XRD. Figure 3 shows the XRD peaks from the GaN/AlN/graphene/SiC sample. Strong intensity from SiC is clearly visible. Additionally, there are a set of peaks that are indexed to first- and second-order reflections of GaN(0002). The position of the GaN peaks confirms that the GaN on graphene has a wurtzite structure and is epitaxial in nature. The XRD rocking curves of GaN(0002) and (0004) peaks are shown in the insets of Fig. 3. The rocking curve full widths at the half maximum (FWHM) of the (0002) and (0004) peaks are 544 and 461 arcsec, respectively. These values are similar to the typical rocking curve FWHM for a 5-μm-thick GaN grown on sapphire substrates, which have a lattice mismatch of 16%.[16] The similarity of these FWHMs for an order of magnitude thinner GaN film may indicate that a better crystalline quality material on EG can be achieved.

In-plane grazing incidence small angle (GISA) and out-of-plane asymmetric XRD measurements were carried out to study epitaxial nature of the GaN on graphene/SiC. In-plane GISA XRD shows that GaN is rotated by 62° with respect to *m*-plane of SiC. The SiC and EG reciprocal lattices are related by a well-known 30° epitaxial relationship.[17] Thus, the ALE AlN is rotated with 30° with respect to EG as shown in Fig. 1(h). Subsequent growth of GaN is in the same orientation as AlN. Few degree differences in the measured value could be due to the strain between III–nitride layers. To confirm the epitaxial nature of GaN on EG, asymmetric diffraction peaks of GaN(21$\bar{3}$3) and SiC(11$\bar{2}$8) were measured as shown in Fig. 4. The XRD rocking curve of GaN(21$\bar{3}$3) has single peak with FWHM of 410 arcsec, which confirms the epitaxial nature of GaN.

Figure 5 shows room-temperature PL spectra of the GaN on EG. There is clearly a near-band-edge (NBE) emission at 3.40 eV and a broad yellow line at 2.27 eV. The NBE emission could result from the free electron–hole pair recombination in GaN, considering its low binding energy of about 20 meV, or band-to-band recombination.[18] The yellow line is believed to be due to the presence of a Ga vacancy and

 © 2013 The Japan Society of Applied Physics

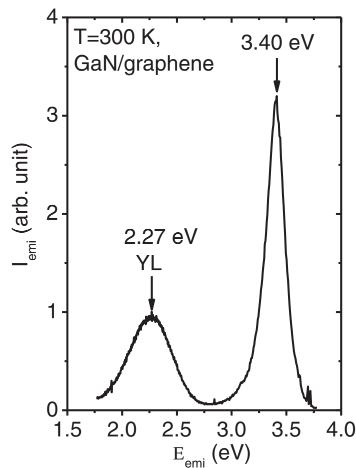

Fig. 5. Room temperature photoluminescence spectra of GaN on AlN/graphene/SiC stack. The near-band-edge emission is at 3.40 eV, and there is a broad yellow line at 2.27 eV due to the presence of a Ga vacancy and oxygen complex point defect.

oxygen complex point defect.[19] Strong intensity of the GaN NBE emission indicates a good optical quality of the GaN/graphene.

The two-step growth (functionalization and low-temperature epitaxy) are the keys to the successful growth of GaN on EG. Currently, the exact mechanism of nucleation is unclear but we believe that the reaction of TMA molecules with surface fluorine that is semi-ionically bonded to carbon in the top graphene layer results in a substitution of aluminum for fluorine and a creation of reaction sites for subsequent AlN growth as shown in Fig. 1(h). XPS measurements after 1.2 nm of ALE AlN growth did not detect fluorine, which supports the claim that the functionalized fluorine simply initiated the ALE growth. The heteroepitaxial growth of GaN on ALE AlN/EG resulted in a less strained, high-crystalline-quality GaN material under optimized growth conditions. Hence, the optimum properties of both GaN and graphene can be utilized for device applications such as HETs.

In conclusion, epitaxial GaN was grown by MOCVD on EG/SiC. The epitaxial nature of these films was enabled by functionalizing the graphene with fluorine prior to a low-temperature, uniform, and pinhole-free ALE AlN nucleation layer. The graphene 2D Raman peak at 2719 cm^{-1} from the GaN/AlN/graphene/SiC stack confirms that the graphene film is preserved after the AlN and GaN subsequent growths. SEM and AFM images show that the GaN is uniform and pinhole-free. The XRD peaks show that the GaN is epitaxial (rotated by 30° with respect to EG) and [0001] oriented with the rocking curve FWHMs of 544, 461, 410 arcsec for (0002), (0004), and $(21\bar{3}3)$ diffraction peaks, respectively. These FWHMs are close to the typical reported values of heteroepitaxially grown state-of-the-art GaN on sapphire. The PL measurement reveals a strong room-temperature band edge emission at 3.40 eV. These results support a successful demonstration of electronic-quality, heteroepitxial wurtzitic GaN on graphene that is currently unavailable and can improve the performance of present state-of-the-art devices such as HETs.

Acknowledgments NN and LON would like to acknowledge the support of the American Society for Engineering Education–Naval Research Laboratory postdoctoral fellowship program. SCH appreciates the support of the National Research Council. This work was supported by the Office of Naval Research.

1) M. Tonouchi, H. Sakai, and T. Kobayashi: Jpn. J. Appl. Phys. **25** (1986) 705.
2) W. R. Deal: IEEE Int. Microwave Symp. (MTT-S) Dig., 2010, p. 1122.
3) Y. Miyamoto, R. Yamamoto, H. Maeda, K. Takeuchi, N. Machida, L. E. Wernersson, and K. Furuya: Jpn. J. Appl. Phys. **42** (2003) 7221.
4) M. Tonouchi, H. Sakai, and T. Kobayashi: Jpn. J. Appl. Phys. **25** (1986) 705.
5) F. J. Kub: U.S Patent Application (2011).
6) W. Mehr, J. Dabrowski, J. C. Scheytt, G. Lippert, Y. H. Xie, M. C. Lemme, M. Ostling, and G. Lupina: IEEE Electron Device Lett. **33** (2012) 691.
7) Y. Sato, K. Itoh, R. Hagiwara, T. Fukunaga, and Y. Ito: Carbon **42** (2004) 3243.
8) V. Wheeler, N. Y. Garces, L. Nyakiti, R. Myers-Ward, G. Jernigan, J. Culbertson, C. R. Eddy, Jr., and D. K. Gaskill: Carbon **50** (2012) 2307.
9) K. Chung, C.-H. Lee, and G.-C. Yi: Science **330** (2010) 655.
10) N. Y. Garces, V. D. Wheeler, and D. K. Gaskill: J. Vac. Sci. Technol. B **30** (2012) 030801.
11) N. Y. Garces, V. D. Wheeler, J. K. Hite, G. G. Jernigan, J. L. Tedesco, N. Nepal, C. R. Eddy, and D. K. Gaskill: J. Appl. Phys. **109** (2011) 124304.
12) H. Zhong, Z. Liu, G. Xu, Y. Fan, J. Wang, X. Zhang, L. Liu, K. Xu, and H. Yang: Appl. Phys. Lett. **100** (2012) 122108.
13) S. M. Bedair, F. G. MvIntosh, J. C. Roberts, E. L. Piner, K. S. Boutros, and N. A. El-Masry: J. Cryst. Growth **178** (1997) 32.
14) S. M. George: Chem. Rev. **110** (2010) 111.
15) B. L. VanMil, R. L. Myers-Ward, J. L. Tedesco, C. R. Eddy, G. G. Jernigan, J. C. Culbertson, P. M. Campbell, J. M. McCrate, S. A. Kitt, and D. K. Gaskill: Mater. Sci. Forum **615–617** (2009) 211.
16) J. N. Kuznia, M. A. Khan, D. T. Olson, R. Kaplan, and J. Freitas: J. Appl. Phys. **73** (1993) 4700.
17) A. J. Van Bommel, J. E. Crombeen, and A. Van Tooren: Surf. Sci. **48** (1975) 463.
18) G. D. Chen, M. Smith, J. Y. Lin, H. X. Jiang, S. H. Wei, M. A. Khan, and C. J. Sun: Appl. Phys. Lett. **68** (1996) 2784.
19) N. Nepal, M. L. Nakarmi, J. Y. Lin, and H. X. Jiang: Appl. Phys. Lett. **89** (2006) 092107.

© 2013 The Japan Society of Applied Physics